A High Sensitivity, Fast Response Optical Fiber Gas Sensor using Micro-drilled Anti-Resonant Fiber

Eleanor A. Warrington [1, 3], Robert Peverall [2], Patrick S. Salter [1], Gus Hancock [2], Martin J. Booth [1], Grant A. D. Ritchie [2] and Julian A. J. Fells [1, 4]

[1] *Department of Engineering Science, University of Oxford, Parks Road, Oxford OX1 3PJ, UK*
[2] *Physical & Theoretical Chemistry Laboratory, South Parks Road, Oxford OX1 3QZ, UK*

[3] *eleanor.warrington@eng.ox.ac.uk*
[4] *julian.fells@eng.ox.ac.uk*

Abstract:
Remote gas detection is often a compromise between high sensitivity and response time. Micro-drilled anti-resonant fiber is used for 0.3% acetylene detection to simultaneously achieve both of these characteristics.

1. Introduction

Highly sensitive gas detection with a fast response time is important for many applications including atmospheric mapping [1], combustion diagnostics [2] and breath composition analysis [3]. The remote sensing capabilities, long-interaction lengths and low loss light confinement [4] of fiber sensors provide high sensitivity and remote detection to aid these applications. However, the response time of the sensor is highly limited by diffusion time and hence slow fiber filling time for a long interaction length. Pressure filling can be used, but this is not always a practical approach for remote sensing [5–9]. Microchannels through the side of hollow-core photonic crystal fiber (PCF) have been used to reduce fiber filling time and hence response time. However, the microchannels damage the guiding structure of the PCF and introduce optical loss. Previous demonstrations of PCF gas sensors show a compromise between sensitivity and response time of the system [10–12]. Shorter path lengths provide a fast response time using low microchannel separation but have low sensitivity [10]. Longer path lengths give higher sensitivity, but the loss of the microchannels dictates a larger microchannel separation and therefore the response time is slower [11, 12]. There is therefore difficulty in simultaneously achieving both high sensitivity and fast response time. In this work, micro-drilled anti-resonant optical fiber (ARF) is used to demonstrate gas detection with both of these attributes simultaneously achieved without the use of a pressure differential.

2. Microchannel Fabrication

The light guidance in ARF is provided by the internal cylindrical structure of hollow capillaries which act as an azimuthal diffraction grating [13, 14]. The gap between capillaries allows for non-destructive, low loss gaseous access to the core, where closely spaced microchannels can be fabricated without introducing excessive optical loss [15, 16]. A series of 15 microchannels (5 × 50 µm dimensions) with a 2 cm separation have been fabricated along a 35 cm sample of ARF, through the fiber cladding and above the gap between the internal capillaries. The ARF used (Exail, IXF-ARF-45-240-V1) is designed for light guidance at 1550 nm. The entire core diameter is 97.11 µm including seven anti-resonant capillaries with a diameter varying around 26 µm and a central core of 22.63 µm. The cladding is approximately 70 µm thick.

A 790 nm femtosecond laser with a pulse duration of 140 fs, a repetition rate of 1 kHz and a 0.5 NA objective lens was used to fabricate the microchannels into the core of the ARF via ultrafast laser ablation [17]. The fiber was orientated about its axis such that the gap between two of the antiresonant capillaries was below the objective lens. Adaptive optics in the form of a spatial light modulator was used for aberration correction when the light was focused into the cylindrical fiber [18].

First, a larger section of cladding to a distance of approximately 65 µm towards the core was removed to create a notch. This was followed by a 5 µm wide microchannel in the center through the remaining cladding. A scanning electron microscope (SEM) image of the microchannel is shown in Figure 1(a) which covers a depth of 50 µm into the fiber. By altering the spacing and geometry of these microchannels, the sensitivity and response time of the fiber system can be altered [19].

(a)

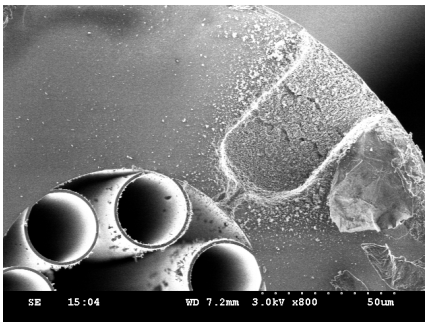

(b)

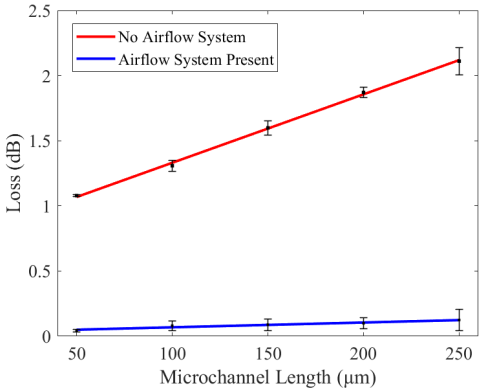

Fig. 1: (a) SEM cross-sectional image of the ablated cladding and fabricated microchannels for the ARF (Exail, IXF-ARF-45-240-V1, 1550 nm), (b) Comparison of the loss measured through the ARF with and without an airflow debris removal system for microchannels of increasing length.

In order to observe the loss introduced by the fabrication of these microchannels into the fiber core, the ARF was spliced to single mode fiber (SMF) with FC/APC connectors for an in-situ, real-time loss measurement. Fusion splicing with standard settings for SMF-SMF were used and the parameters adapted to include fiber overlap, similarly to Min *et al.* [20]. The coupling loss was recorded to be on average 5.25 dB per splice with a $\pm$ 1 dB polarization dependence.

Any debris caused by the cladding ablation should be removed before microchannel fabrication to avoid a scattering effect in the core. The first method involved using the ultrafast laser ablation to eject any material present in the initial notch. However, using this method, and upon measurement of the optical loss and imaging of the cross section, it was clear that debris had entered the core. An airflow system was therefore installed to provide additional force for debris removal and the loss was subsequently significantly reduced, as shown in Figure 1(b). Microchannels of increasing length were fabricated to show the effect on the loss of the presence of the microchannel. Each channel remained at a width of approximately 5 μm. The low loss results show the possibility of fabricating closely spaced microchannels along long lengths of fiber without compromising on loss, giving the desired characteristics of a fast response time with high sensitivity.

3. Wavelength Modulation Spectroscopy

To increase the sensitivity of the gas sensor, wavelength modulation spectroscopy (WMS) was carried out to detect the strong near-IR absorption lines of acetylene using a 1532 nm semiconductor laser with current tuning of 0.65 GHz/mA. This technique involves imposing both slow and fast modulation on the central laser frequency. A sample of 0.3% acetylene / 0.3% methane balanced in air was used and the central frequency of the laser was slowly tuned through the absorption feature using a current ramp, provided by a function generator. A lock-in amplifier supplied the fast modulation with a frequency of 17.48 kHz. This had the form of a sinusoid with an amplitude of 0.072 GHz and was imposed on the slowly varying ramp function [21]. The peak to valley width of the first harmonic was measured to be 2.10 GHz, consistent with a typical atmospheric pressure broadened spectral linewidth of a few GHz. Hence, the magnitude of the variation in optical frequency is small in comparison, a key feature of the WMS technique. This fast sinusoidal frequency modulation was mapped to a variation in intensity when the central wavelength was slowly scanned through the absorption feature [22]. The resulting signal on the photodetector was demodulated by the lock-in amplifier and different harmonics of the fast modulation frequency were produced. This technique is advantageous as the detection is shifted to higher frequencies where all excess noise is usually reduced. The central wavelength was set to 1531.59 nm (6529.17 cm^{-1}) to target a P branch, J = 11 ro-vibrational transition. This is a combination band of two quanta of C - H stretches in C_2H_2. The integrated cross section is equal to 1.165 $\times 10^{-20}$ $cm^2 cm^{-1}$ [23].

The machined ARF was connected to the laser via butt coupling to a SMF as illustrated in Figure 2(a) and was mounted in front of a 20$\times$ 0.4 NA objective lens and a photodiode with a 20 dB neutral density filter to reduce light intensity and hence avoid saturation. Etalon effects within the optical system were mitigated by purposeful angular misalignment of the components. The pressure of the gas box was reduced to 4 Torr and repressurized with the 0.3% acetylene gas sample. At 500 Torr, the well defined first harmonic, in Figure 2(b), was observed.

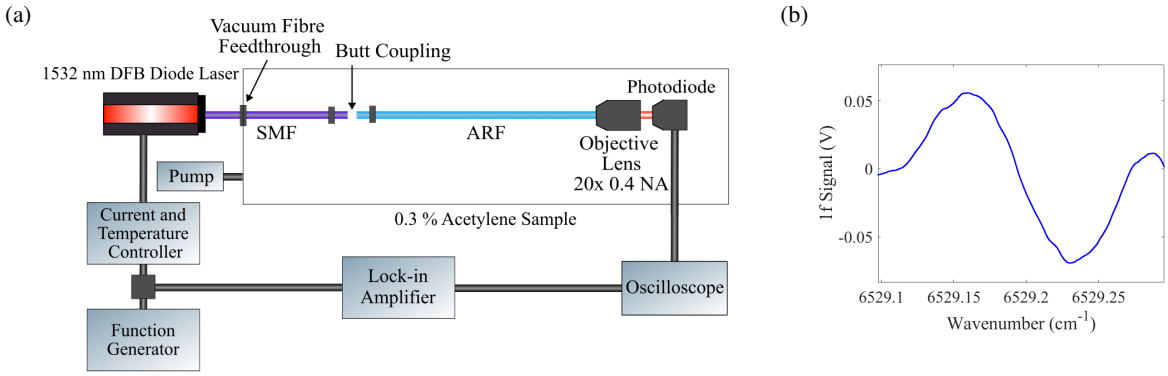

Fig. 2: (a) Experimental setup used for WMS with the machined 35 cm ARF present in a 0.3% acetylene gas sample, (b) Detection of the first harmonic for the P(11e), 1531.59 nm (6529.17 cm^{-1}) ro-vibrational transition of acetylene.

3.1. Time Response

In order to determine the time response of the system, the 0.3% acetylene gas sample was injected into the box at atmospheric pressure and the signal was recorded after each average of 100 scans. This corresponds to 10 second intervals at a 10 Hz trigger rate. The response time of the system is therefore estimated by the recorded time stamp of the first scan with a non-zero first harmonic amplitude. Inversely, a pump was used to flush air through the box to remove the acetylene and the data recorded as the signal decreased. The results of this are shown in Figure 3. The data points were found to fluctuate due to baseline noise.

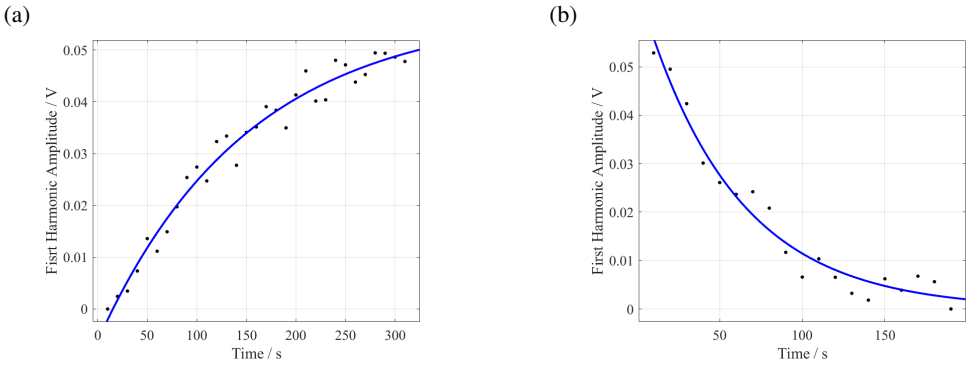

Fig. 3: First harmonic amplitude recorded with scans saved every 100 averages, (a) Recorded as the mixture of 0.3% acetylene / 0.3% methane balanced in air is inserted into the vacuum box, (b) Recorded as the box is returned to a vacuum via a pump.

The recorded time response of the gas sensor is a combination of the time for the gas to fill the chamber and the fiber filling time tempered by the speed with which the oscilloscope can average out the noise to allow a first harmonic to be identified. This last quantity can be reduced by limiting the number of averages in a scan, but this must be balanced with the identification of the harmonic above the noise level. In this measurement, these effects cannot be readily deconvolved, however both the signal response times in Figure 3 are consistent with the expected chamber filling and pump through times. It is therefore surmised, considering (on a gas diffusion scale) the large size of the microchannels, that the fiber response time could be considerably faster than this, in this case $\ll 10$ s. Clearly, the demonstration could be improved by encasing the fiber in a glass tube with an inlet value to allow for very fast filling of the atmosphere surrounding the fiber such that the response time of the system is dominated by the fiber filling time. The first harmonic was already detected at the first recorded scan, taken after 100 averages in around 10 s.

3.2. Detection Limit

The detection limit was determined by the signal-to-noise ratio (SNR) where the noise is given by the standard deviation of the baseline, far away from the first harmonic. The SNR was found to be equal to 11.92 with a standard

deviation of 0.018 V. For the 3000 ppm acetylene gas mixture, the detection limit is therefore equal to 252 ppm. With comparison to results shown in the literature, for the length scales of 0.1 m of fiber, this is a promising result for a fiber gas sensor with both high sensitivity and fast response time, without the use of a pressure differential. However, it must be noted the detection limit will be affected by the chosen gas species.

4. Conclusion

This work has demonstrated a hollow-core optical fiber gas sensor with simultaneous high sensitivity and fast response time. This was achieved using 35 cm of anti-resonant hollow core fiber with a series of 15 holes micro-drilled in the side. Femtosecond laser ablation was used to fabricate through the capillary gap into the hollow fiber core. Measurements on 0.3% acetylene gas showed a detection limit of 252 ppm, and a fast response time of $\ll 10$ s. There is potential to scale up to longer ARF samples, whilst maintaining the low loss, closely spaced microchannels, further reducing the detection limit without compromising on response time.

References

1. J. B. McManus *et al.*, "Recent progress in laser-based trace gas instruments: performance and noise analysis," Appl. Phys. B. **119**, 203-218 (2015)
2. R. N. Zare *et al.*, "High-precision optical measurements of $^{13}C/^{12}C$ isotope ratios in organic compounds at natural abundance" in *Proc. of the National Academy of Science* 106 (27), 10928 - 10932 (2009)
3. V. L. Kasyutich, and P. A. Martin, "$^{13}CO_2/^{12}CO_2$ isotopic ratio measurements with a continuous-wave quantum cascade laser in exhaled breath," Infrared Phys. Technol. **55**, 60-66 (2012)
4. F. Yu and J. C. Knight, "Negative Curvature Hollow-Core Optical Fiber," IEEE J. Sel. Top. Quantum Electron. **22** (2), 146-155 (2016)
5. M. Nikodem *et al.*,"Laser absorption spectroscopy at 2 μm inside revolver-type anti-resonant hollow core fiber," Opt. Express **27** (10), 14998 - 15006 (2019)
6. P. Jaworski *et al.*,"Antiresonant Hollow-Core Fiber-Based Dual Gas Sensor for Detection of Methane and Carbon Dioxide in the Near- and Mid-Infrared Regions," Sensors **20** (14), 3813 (2020)
7. P. Jaworski *et al.*, "Nitrous oxide detection at 5.26 μm with a compound glass antiresonant hollow-core optical fiber," Opt. Lett. **45** (6), 1326 - 1329 (2020)
8. C. Yao *et al.*,"Sub-ppm CO detection in a sub-meter-long hollow-core negative curvature fiber using absorption spectroscopy at 2.3 μm," Sens. Actuators B Chem. **303**, (2020)
9. M. Nikodem *et al.*, "Demonstration of mid-infrared gas sensing using an anti-resonant hollow core fiber and a quantum cascade laser," Opt. Express **27** (25), 36350 - 36357 (2019)
10. Y. L. Hoo *et al.*,"Fast Response Microstructured Optical Fiber Methane Sensor With Multiple Side-Openings," IEEE Photon. Technol. Lett. **22** (5), 296-298 (2010)
11. J. P . Carvalho *et al.*,"Remote System for Detection of Low-Levels of Methane Based on Photonic Crystal Fibres and Wavelength Modulation Spectroscopy," J. Sens. **2009**, (2009)
12. J. P. Parry *et al.*, "Towards practical gas sensing with micro-structured fibres," Meas. Sci. Technol. **20** (7), 075301 (2009)
13. A. D. Pryamikov,"Negative curvature hollow core fibers: design, fabrication, and applications" in *Proc. of SPIE LASE* 8961, SF, CA, United States, (2014)
14. A. D. Pryamikov *et al.*, "Demonstration of a waveguide regime for a silica hollow - core microstructured optical fiber with a negative curvature of the core boundary in the spectral region > 35 μm," Opt. Express **19** (2), 1441-1448 (2011)
15. P. Kozioł *et al.*, "Fabrication of Microchannels in a Nodeless Antiresonant Hollow-Core Fiber Using Femtosecond Laser Pulses," Sensors **21** (22), 7591 (2021)
16. C. C. Novo *et al.*, "Femtosecond laser machining of hollow-core negative curvature fibres," Opt. Express **28** (17), 25491 - 25501 (2020)
17. B. N. Chichkov *et al.*, "Femtosecond, picosecond and nanosecond laser ablation of solids," Appl. Phy. A **63** (2), 109-115 (1996)
18. P. S. Salter *et al.*,"Femtosecond fiber Bragg grating fabrication with adaptive optics aberration compensation," Opt. Lett. **43** (24), 5993-5996 (2018)
19. J. Karp *et al.*,"Fugitive methane leak detection using mid-infrared hollow-core photonic crystal fiber containing ultrafast laser drilled side-holes" in *Proc. SPIE 9852, Fiber Optic Sensors and Applications XIII*, 985210 (2016)
20. Y. Min *et al.*, "Fusion Splicing of Silica Hollow Core Anti-Resonant Fibers With Polarization Maintaining Fibers," J. Light. Technol. **39** (10), 3251-3259 (2021)
21. Y. Ma *et al.*, "Hollow-core anti-resonant fiber based light-induced thermoelastic spectroscopy for gas sensing," Opt. Express **30** (11), 18836-18844 (2022)
22. S. Schilt *et al.*, "Wavelength Modulation Spectroscopy: Combined Frequency and Intensity Laser Modulation," Appl. Opt. **42** (33), 6728-6738 (2003)
23. I. E. Gordon *et al.*, "The HITRAN2020 molecular spectroscopic database," J. Quant. Spectrosc. Radiat. Transf. **277**, 107949 (2022)